

Enhancement of the upconversion radiation in $\text{Y}_2\text{O}_3 : \text{Er}^{3+}$ nanocrystals by codoping with Li^+ ions

G. Y. Chen, H. C. Liu, G. Somesfalean, Y. Q. Sheng, H. J. Liang, Z. G. Zhang, Q. Sun, and F. P. Wang

Citation: [Applied Physics Letters](#) **92**, 113114 (2008); doi: 10.1063/1.2901039

View online: <http://dx.doi.org/10.1063/1.2901039>

View Table of Contents: <http://scitation.aip.org/content/aip/journal/apl/92/11?ver=pdfcov>

Published by the [AIP Publishing](#)

Articles you may be interested in

[Intense upconversion and infrared emissions in \$\text{Er}^{3+} - \text{Yb}^{3+}\$ codoped \$\text{Lu}_2\text{SiO}_5\$ and \$\(\text{Lu}_{0.5}\text{Gd}_{0.5}\)_2\text{SiO}_5\$ crystals](#)

Appl. Phys. Lett. **93**, 011110 (2008); 10.1063/1.2954010

[Demonstration of enhanced population feeding of the 1.53 \$\mu\text{m}\$ emitting level of \$\text{Er}^{3+}\$ in \$\text{TeO}_2 - \text{WO}_3 - \text{Li}_2\text{O} - \text{P}_2\text{O}_5\$ glasses using upconversion luminescence spectroscopy](#)

J. Appl. Phys. **103**, 063107 (2008); 10.1063/1.2891788

[Optical thermometry through infrared excited green upconversion emissions in \$\text{Er}^{3+} - \text{Yb}^{3+}\$ codoped \$\text{Al}_2\text{O}_3\$](#)

Appl. Phys. Lett. **90**, 181117 (2007); 10.1063/1.2735955

[Judd-Ofelt analysis of spectroscopic property of \$\text{Er}^{3+}\$ in congruent and near-stoichiometric \$\text{Zn} - \text{Er}\$ -codoped \$\text{LiNbO}_3\$ crystals](#)

J. Appl. Phys. **101**, 053523 (2007); 10.1063/1.2654162

[Upconversion luminescence, intensity saturation effect, and thermal effect in \$\text{Gd}_2\text{O}_3 : \text{Er}^{3+}, \text{Yb}^{3+}\$ nanowires](#)

J. Chem. Phys. **123**, 174710 (2005); 10.1063/1.2087487



Re-register for Table of Content Alerts

Create a profile.



Sign up today!



Enhancement of the upconversion radiation in $Y_2O_3:Er^{3+}$ nanocrystals by codoping with Li^+ ions

G. Y. Chen,¹ H. C. Liu,¹ G. Somesfalean,¹ Y. Q. Sheng,¹ H. J. Liang,¹ Z. G. Zhang,^{1,a)} Q. Sun,² and F. P. Wang²

¹Department of Physics, Harbin Institute of Technology, 150001 Harbin, People's Republic of China

²Department of Applied Chemistry, Harbin Institute of Technology, 150001 Harbin, People's Republic of China

(Received 28 September 2007; accepted 28 February 2008; published online 21 March 2008)

We report on an innovative route to increase the upconversion (UC) green radiation by two orders of magnitude in $Y_2O_3:Er^{3+}$ nanocrystals through tailoring Er^{3+} ions' local environment with Li^+ ions under diode laser excitation of 970 nm. Theoretical investigations based on the steady-state rate equations indicate that such enhancement arises from a combining effect of the tailored lifetime of the intermediate $^4I_{11/2}(Er)$ state, the suppressed cross relaxation $^2H_{11/2}(Er) + ^4I_{15/2}(Er) \rightarrow ^4I_{9/2}(Er) + ^4I_{13/2}(Er)$ process, and the enlarged nanocrystal size induced by the Li^+ ions. The proposed route here may constitute a promising step to solve the low efficiency problem in UC materials. © 2008 American Institute of Physics. [DOI: 10.1063/1.2901039]

Unlike multiphoton absorption in organic dyes or semiconductor quantum dots, photon upconversion (UC) involves real intermediate quantum states to generate efficient visible light by near infrared (NIR) excitation.^{1–5} Insufficient intensity, however, constitutes still the main limitation for the practical applications of UC materials, especially rare-earth-ion-doped inorganic nanocrystals,^{2,6,7} in the fields of UC lasers,⁸ flat-panel displays,⁹ light-emitting diodes,¹⁰ temperature sensors,¹¹ biolabels,^{12–14} DNA detection,¹⁵ photodynamic therapy (PDT),^{7,16} etc. Unfortunately, ever since the first report by Auzel in the 1960s on UC enhancement through Yb^{3+} sensitization,¹⁷ there have been no strategies to increase the UC fluorescence by orders of magnitude. Therefore, it will be of significance to develop new routes to greatly increase the UC emissions in order to meet their practical application requirements.

It is well known that the intra- $4f$ electronic transitions of rare-earth ions are parity forbidden, and become partially allowed when intermixing the f states with higher electronic configurations enabled by the local columbic field of host lattice.^{1–3,18} Hence, the tailoring rare-earth ions' local environment in the host lattice can constitute a promising route to enhance their Stokes and anti-Stokes luminescences. The Li^+ ion is the smallest metallic ion in the periodic table and has the smallest cationic radius, which is favorable for its movement and localization in the host lattice. Consequently, the Li^+ ion is an ideal cationic ion for tailoring the local crystal field of rare-earth ions. In this letter, we primarily report on an innovative route to increase the UC green radiation by two orders of magnitude in $Y_2O_3:Er^{3+}$ nanocrystals via codoping with Li^+ ions.

Yttrium oxide (Y_2O_3) nanocrystals were selected here due to the intriguing chemical and optical properties of host lattice, e.g., high thermal conductivity and expansion coefficient, broad transparency range of 0.23–8 μm , relatively low phonon energy (maximum 600 cm^{-1}), etc.^{19,20} Moreover, the UC emissions of $Y_2O_3:Er^{3+}$ nanocrystals have been well characterized by pumping the intermediate $^4I_{11/2}$ state of

the Er^{3+} ion via a facile 970 nm NIR diode laser.^{5,20} Additionally, $Y_2O_3:Er^{3+}$ nanocrystals have been employed for background-free fluorescent imaging¹⁴ and deep tumor treatment via PDT photosensitizer excitation,⁷ since the 970 nm excitation wavelength is fairly transparent for most large biomolecules.⁷

Nanocrystals Y_2O_3 doped with 1 mol % Er^{3+} ions and 0, 3, 5, 7, 10, and 15 mol % Li^+ ions were prepared via a previous procedure with a small difference by replacing yttrium nitrate with appropriate lithium nitrate.^{13,19} Details for the UC fluorescence recording were described elsewhere.¹³ Decay profiles of the 1015 nm radiation were measured by square-wave modulation of the electric current input to the 970 nm diode laser, and by recording the signals via a Tektronix TDS 5052 digital oscilloscope with a lock-in preamplifier (Stanford Research System Model SR830 DSP) employing a chopping rate of 3000 rps. A NIR-sensitive InGaAs photodiode (Thorlabs, DET 410/M) was used for measuring the decay profiles and fluorescence spectra of the NIR light. X-ray diffraction (XRD) experiment evidenced that all the prepared Y_2O_3 powders are of cubic structure and the codoping of Li^+ ions can tailor the crystal field of the Y_2O_3 lattice. The average sizes of nanocrystals Y_2O_3 codoped with 0, 3, 5, 7, 10, and 15 mol % Li^+ ions, according to Scherrer's equation,¹⁹ were calculated to be about 36, 54, 58, 58, 58, and 58 nm, respectively.

Figure 1 displays the green UC emission of the $^2H_{11/2}/^4S_{3/2} \rightarrow ^4I_{15/2}$ transition in Y_2O_3 nanocrystals doped with 1 mol % Er^{3+} ions and various Li^+ ions under 970 nm diode laser excitation.²⁰ The inset illustrates the intensity ratio of the green to red as a function of Li^+ ions. The weak red UC radiation of the $^4F_{9/2} \rightarrow ^4I_{15/2}$ transition were not shown here, since we focus on the increase in the dominant green UC radiation.²⁰ As shown in Fig. 1, the fluorescence dramatically increases with Li^+ ions of 0–5 mol %, and remains about the same at higher concentrations. The maximum enhancement for the suboptimized experimental conditions presented here were measured to be about 45–75 times (measurement error 20%) corresponding to Li^+ ions of 5 mol % under a variety of excitation conditions. The variance of the

^{a)}Electronic mail: zhangzhiguo@hit.edu.cn.

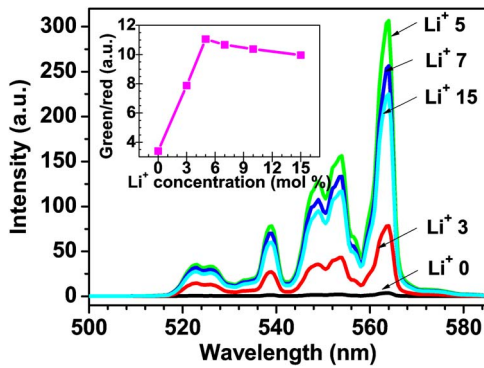


FIG. 1. (Color online) Measured UC green emission in Y_2O_3 nanocrystals doped with 1 mol % Er^{3+} ions and various Li^+ ions under diode laser excitation of 970 nm. The inset is the intensity ratio of the green to red as a function of Li^+ ions.

enhancement times may arise from the fact that the total fluorescence spectral distribution is dependent on the pump power, as demonstrated in $\text{NaYF}_4:\text{Yb}^{3+}/\text{Er}^{3+}$ nanocrystals.²¹ The enhancement results here illustrate that tailoring Er^{3+} ions' local environment via Li^+ ions indeed can significantly favor the UC output, which was further confirmed by replacing Li^+ ions with other nonluminescent ions such as Na^+ , K^+ , and Zn^{2+} .

Figure 2 presents the UC mechanisms of the green and red emissions.^{9,20} The Er^{3+} ion can be promoted to the $^4I_{11/2}$ state through ground state absorption (GSA) of laser photons, and then to the $^4F_{7/2}$ state by use of the excited state absorption (ESA) 1 or energy transfer UC (ETU) 1 processes. Alternatively, the Er^{3+} ion at the $^4I_{11/2}$ state can non-radiatively relax to the $^4I_{13/2}$ state, and is further excited to the $^4F_{9/2}$ state by ESA 2 or ETU 2 processes. The $^4F_{9/2}$ state can also be populated by multiphonon-assisted relaxations from the upper $^2H_{11/2}/^4S_{3/2}$ state. It is noted that such two processes for the red UC generation are independent of Er^{3+} ion's distribution in the host lattice, while the cross relaxation (CR) process for populating the $^4I_{13/2}$ state (further to the $^4F_{9/2}$ state) depends on the Er^{3+} ion's distribution and the population in the $^2H_{11/2}/^4S_{3/2}$ state.

To simply theoretical calculations for the green UC enhancement, it is reasonable to neglect the red UC emission due to the much lower intensity than the green one.^{5,22} The steady-state rate equations can thereby be expressed as follows:

$$\frac{dN_2}{dt} = 0 = R_1 N_0 - R_2 N_2 - 2CN_2^2 - N_2/\tau_2, \quad (1)$$

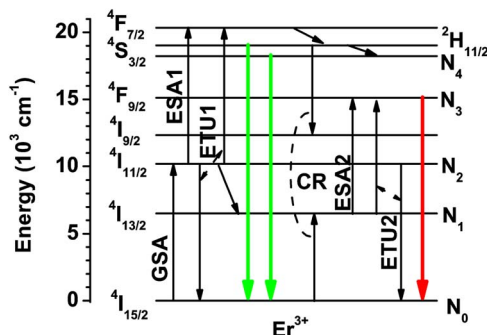


FIG. 2. (Color online) Energy level diagram of Er^{3+} ion as well as the UC mechanisms for the green and red emissions.

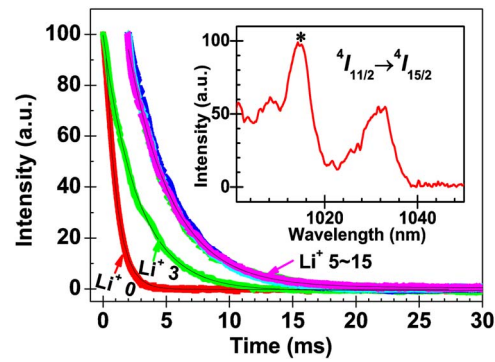


FIG. 3. (Color online) Decay profiles of the $^4I_{11/2} \rightarrow ^4I_{15/2}$ transition in Y_2O_3 nanocrystals doped with 1 mol % Er^{3+} ions and 0, 3, 5, 7, 10, and 15 mol % Li^+ ions. The inset is the fluorescence spectrum of the $^4I_{11/2} \rightarrow ^4I_{15/2}$ transition in the range of 1000–1050 nm under diode laser excitation of 970 nm.

$$\frac{dN_4}{dt} = 0 = R_2 N_2 + CN_2^2 - N_4/\tau_4, \quad (2)$$

$$N = N_0 + N_2 + N_4, \quad (3)$$

$$I_{\text{green}} = \beta_{\text{green}} N_4 h\nu_{\text{green}}/\tau_4, \quad (4)$$

where $N_i(\tau_i)$ is the energy level populations (decay time) denoted in Fig. 2, R_1 and R_2 are the rates of GSA and ESA 1 processes, respectively, which are constant here due to the identical excitation condition,⁸ C is the coefficient of ETU 1 process, and β_{green} is the ratio of the radiation rate to the decay rate in the $^2H_{11/2}/^4S_{3/2}$ state. If $N \approx N_0$, $R_2 N_2 + 2CN_2^2 \ll N_2/\tau_2$,²² we can easily get from Eqs. (1)–(4) that

$$I_{\text{green}} = \beta_{\text{green}} (\tau_2 R_1 R_2 N + C \tau_2^2 R_1^2 N^2) h\nu_{\text{green}} \approx \beta_{\text{green}} h\nu_{\text{green}} C \tau_2^2 R_1^2 N^2. \quad (5)$$

The approximation in Eq. (5) arises from the fact that the ETU 1 process is supposed to dominate over the ESA 1 process, which can illustrate well the observed enhancement results. According to Eq. (5), the increase in the parameters τ_2 and β_{green} can lead the green UC radiation to increase, in good agreement with the discussion results in Ref. 8.

Figure 3 displays the decay profiles of the $^4I_{11/2} \rightarrow ^4I_{15/2}$ transition at 1015 nm in Y_2O_3 nanocrystals doped with 1 mol % Er^{3+} ions and 0–15 mol % Li^+ ions. The inset presents the spectrum for the $^4I_{11/2} \rightarrow ^4I_{15/2}$ transition in nanocrystals Y_2O_3 codoped with 5 mol % Li^+ ions under diode laser excitation of 970 nm, which agrees well with the previous data.³ According to Fig. 3, the lifetime of the intermediate $^4I_{11/2}$ state were measured to be 0.8(2) ms and 2.7(3) ms for 0 and 3 mol % Li^+ ions, respectively, and to be all about 3.4(3) ms for Li^+ ions higher than 5 mol %. These data indicate that the local crystal field around Er^{3+} ions was gradually tailored for Li^+ ions of 0–5 mol % and becomes nearly identical at higher Li^+ ions. According to Eq. (5), the large and slight increases in lifetime τ_2 for Li^+ ions of 0–3 and 3–5 mol % will lead to great and small fluorescence increases, respectively. The unchanged lifetime for higher Li^+ ions will result in a nearly constant enhancement. Such conclusions agree well with the experimental observations in Fig. 1. It should be noted that the linear increase in parameter β_{green} for Li^+ ions of 0–5 mol % will further enlarge the enhancement difference (see below). Quantitatively, for example, the maximum 4.2 times lifetime increase for Li^+ ions

of 5 mol % can lead to about 18 times fluorescence increase, which falls short for the 45–75 times enhancement observed.

It is obvious from the inset of Fig. 1 that the intensity ratio of the green to red linearly increases for Li⁺ ions up to 5 mol %, and then remains constant at around 10 for higher Li⁺ ions. According to Fig. 2, for the constant Er³⁺ ions here, there should be a constant value for the intensity ratio, which contradicts the experimental results. Moreover, a much larger population in the ²H_{11/2}/⁴S_{3/2}(Er) state induced by Li⁺ ions should favor the CR population of the ⁴I_{13/2}(Er) state, thereby reducing the green to red ratio. Consequently, the linear increase in the intensity ratio indicates that Li⁺ ions can dissociate the Er³⁺ clusters in the Y₂O₃ crystal lattice, thus, hampering the red emission by avoiding the CR process in Fig. 3. It is noted that the parameter β_{green} directly relates to the CR process and the red emission, of which the hindrance can lead the parameter β_{green} to increase. As can be evaluated from the green to red ratio, the parameter β_{green} is increased about 3 times by dissociating the Er³⁺ clusters, which according to Eq. (5) will lead the green emission to increase further about 3 times for Li⁺ ions of 5 mol %.

It is worthwhile to point out that the increased nanocrystal size (see XRD results) induced by Li⁺ ions can also contribute to the green UC enhancement, since the larger nanocrystal size will have less effect of surface contaminations and defects on the embedded rare-earth ions.²⁰ Unfortunately, such enhancement cannot be calculated, which may be evaluated by the fall short for the experimental observation.

The key mechanism for the UC enhancement arises from the fact that the codoping of Li⁺ ions can tailor the local crystal field around the Er³⁺ ions. The tailored local crystal field will interact with Er³⁺ ion, slightly modify its wave functions, and eventually alter the radiation properties of the intermediate ⁴I_{11/2} state. It is noted that the radiation parameters of ⁴I_{11/2} state directly relate to the green fluorescence intensity. As presented in this letter, the lengthening of its lifetime can lead the UC fluorescence to be increased by one order of magnitude. It is worthwhile to mention that the modified UC pathways and the increased nanocrystal size also contribute to the fluorescence enhancement, but not very significantly.

In summary, we have demonstrated an innovative route to enhance the green UC emission by about two orders in Y₂O₃:Er³⁺ nanocrystals through tailoring Er³⁺ ions' local environment with nonluminescent Li⁺ ions. Although the pro-

posed route was demonstrated here in Er³⁺-doped Y₂O₃ nanocrystals, it may directly apply to other rare-earth ions (e.g., Ho³⁺ and Tm³⁺) and other UC materials (e.g., oxide and fluoride crystals, fibers, films, etc), since the strategy is based on a fundamental consideration.

The work is supported by the SIDA Asian-Swedish Research Partnership Programme and the 863 Hi-Tech Research and Development Program of People's Republic of China.

- ¹F. Auzel, *Chem. Rev. (Washington, D.C.)* **104**, 139 (2004).
- ²J. F. Suyver, A. Aebischer, D. Biner, P. Gerner, J. Grimm, S. Heer, K. W. Krämer, C. Reinhard, and H. U. Güdel, *Opt. Mater. (Amsterdam, Neth.)* **27**, 1111 (2005).
- ³F. Vetrone, J. C. Boyer, J. A. Capobianco, A. Speghini, and M. Bettinelli, *J. Phys. Chem. B* **107**, 1107 (2003).
- ⁴E. De la Rosa-Cruz, L. A. Díaz-Torres, R. A. Rodríguez-Rojas, M. A. Meneses-Nava, and O. Barbosa-García, *Appl. Phys. Lett.* **83**, 4903 (2003).
- ⁵D. Matsuura, *Appl. Phys. Lett.* **81**, 4526 (2002).
- ⁶S. Sivakumar, F. C. J. M. van Veggel, and P. Stanley May, *J. Am. Chem. Soc.* **129**, 620 (2007).
- ⁷P. N. Prasad, *Introduction To Biophotonics* (Wiley, New York, 2003), Chap. 12 and 15.
- ⁸R. Scheps, *Prog. Quantum Electron.* **20**, 271 (1996).
- ⁹F. Liu, E. Ma, D. Q. Chen, Y. L. Yu, and Y. S. Wang, *J. Phys. Chem. B* **110**, 20843 (2006).
- ¹⁰S. Sivakumar, F. C. J. M. van Veggel, and M. Raudsepp, *J. Am. Chem. Soc.* **127**, 12464 (2005).
- ¹¹B. Dong, D. P. Liu, X. J. Wang, T. Yang, S. M. Miao, and C. R. Li, *Appl. Phys. Lett.* **90**, 181117 (2007).
- ¹²J. C. Boyer, L. A. Cuccia, and J. A. Capobianco, *Nano Lett.* **7**, 847 (2007).
- ¹³G. Y. Chen, Y. G. Zhang, G. Somesfalean, Z. G. Zhang, Q. Sun, and F. P. Wang, *Appl. Phys. Lett.* **89**, 163105 (2006).
- ¹⁴S. F. Lim, R. Riehn, W. S. Ryu, N. Khanarian, C. K. Tung, D. Tank, and R. H. Austin, *Nano Lett.* **6**, 169 (2006).
- ¹⁵L. Y. Wang and Y. D. Li, *Comput. Chem. Eng.* **24**, 2557 (2006).
- ¹⁶P. Zhang, W. Steelant, M. Kumar, and M. Scholfield, *J. Am. Chem. Soc.* **129**, 4526 (2007).
- ¹⁷F. Auzel, *Acad. Sci., Paris, C. R.* **262**, 1016 (1966).
- ¹⁸A. Patra, C. S. Friend, R. Kapoor, and P. N. Prasad, *Appl. Phys. Lett.* **83**, 284 (2003).
- ¹⁹G. Y. Chen, G. Somesfalean, Z. G. Zhang, Q. Sun, and F. P. Wang, *Opt. Lett.* **32**, 87 (2007).
- ²⁰F. Vetrone, J. C. Boyer, J. A. Capobianco, A. Speghini, and M. Bettinelli, *Chem. Mater.* **15**, 2737 (2003).
- ²¹J. F. Suyver, J. Grimm, K. W. Krämer, and H. U. Güdel, *J. Lumin.* **114**, 53 (2005).
- ²²M. Pollnau, D. R. Gamelin, S. R. Lüthi, H. U. Güdel, and M. P. Hehlen, *Phys. Rev. B* **61**, 3337 (2000).